
Predictive Neural Networks

Frieder Stolzenburg¹ Olivia Michael² Oliver Obst²

Abstract

Recurrent neural networks are a powerful means to cope with time series. We show that already linearly activated recurrent neural networks can approximate any time-dependent function $f(t)$ given by a number of function values. The approximation can effectively be learned by simply solving a linear equation system; no backpropagation or similar methods are needed. Furthermore, the network size can be reduced by taking only the most relevant components of the network. Thus, in contrast to others, our approach not only learns network weights but also the network architecture. The networks have interesting properties: In the stationary case they end up in ellipse trajectories in the long run, and they allow the prediction of further values and compact representations of functions. We demonstrate this by several experiments, among them multiple superimposed oscillators (MSO) and robotic soccer. Predictive neural networks outperform the previous state-of-the-art for the MSO task with a minimal number of units.

1. Introduction

Deep learning in general means a class of machine learning algorithms that use a cascade of multiple layers of nonlinear processing units for feature extraction and transformation (Deng & Yu, 2014). The tremendous success of deep learning in diverse fields such as computer vision and natural language processing seems to depend on a bunch of ingredients: artificial, possibly recurrent neural networks (RNNs) with nonlinearly activated neurons, convolutional layers, and iterative training methods like backpropagation (Goodfellow et al., 2016). But which of these components are really essential for machine learning tasks such as time-

series prediction?

Research in time series analysis and hence modeling dynamics of complex systems has a long tradition and is still highly active due to its crucial role in many real-world applications (Lipton et al., 2015) like weather forecast, stock quotations, comprehend trajectories of objects and agents, or solving number puzzles (Ragni & Klein, 2011; Glüge & Wendemuth, 2013). The analysis of time series allows among others 1. data compression, i.e., compact representation of time series, e.g., by a function $f(t)$, and 2. prediction of further values.

Numerous research addresses these topics by RNNs, in particular variants of networks with long short-term memory (LSTM) (cf. Hochreiter & Schmidhuber, 1997). But the question remains what can already be done with simple artificial neural networks. In the following, we therefore consider an alternative, very simple type of RNN which we call predictive neural network (PrNN). It only uses linear activation and attempts to minimize the network size. Thus in contrast to other approaches not only network weights but also the network architecture is learned.

The rest of the paper is structured as follows: First we briefly review related works (Sect. 2). We then introduce PrNNs as a special and simple kind of RNNs together with their properties, including the general network dynamics and their long-term behavior (Sect. 3). Afterwards, learning PrNNs is explained (Sect. 4). It is a relatively straightforward procedure which allows network reduction; no backpropagation or gradient descent method is needed. We also discuss results and experiments (Sect. 5). The paper ends up with conclusions (Sect. 6).

2. Related Works

Simple RNNs were proposed by Elman (1990). By allowing them to accept sequences as inputs and outputs rather than individual observations, RNNs extend the standard feedforward multilayer perceptron networks. As shown in many sequence modeling tasks, data points such as video frames, audio snippets and sentence segments are usually highly related in time. This results in RNNs being used as the indispensable tools for modeling such temporal dependencies. Linear RNNs and some of their properties (like short-term memory) are already investigated by White et al. (1994).

¹Department of Automation and Computer Sciences, Harz University of Applied Sciences, Friedrichstr. 57-59, 38855 Wernigerode, Germany ²Centre for Research in Mathematics, Western Sydney University, Locked Bag 1797, Penrith NSW 2751, Australia. Correspondence to: Frieder Stolzenburg <fstolzenburg@hs-harz.de>, Oliver Obst <o.obst@westernsydney.edu.au>.

Unfortunately, however, it can be a struggle to train RNNs to capture long-term dependencies (see [Bengio et al., 1994](#); [Pascanu et al., 2013](#)). This is due to the gradients vanishing or exploding during backpropagation, which in turn makes the gradient-based optimization difficult.

Nowadays, probably the most prominent and dominant type of RNNs are long short-term memory (LSTM) networks ([Hochreiter & Schmidhuber, 1997](#)). The expression “long short-term” refers to the fact that LSTM is a model for the short-term memory which can last for a long period of time. An LSTM is well-suited to classify, process and predict time series given time lags of unknown size. They were developed to deal with the exploding and vanishing gradient problem when training traditional RNNs (see above). A common LSTM unit is composed of a cell, an input gate, an output gate, and a forget gate. Each unit type is activated in a different manner, whereas in this paper we consider completely linearly activated RNNs.

Echo state networks (ESNs) play a significant role in RNN research as they provide an architecture and supervised learning principle for RNNs. They do so by driving a random, large, fixed RNN, called *reservoir* in this context, with the input signal, which then induces in each neuron within this reservoir network a nonlinear response signal. They also combine a desired output signal by a trainable linear combination of all of these response signals ([Jaeger, 2007; 2014](#)). [Xue et al. \(2007\)](#) propose a variant of ESNs that work with several independent (decoupled) smaller networks.

[Hu & Qi \(2017\)](#) have proposed a novel state-frequency memory (SFM) RNN, which aims to model the frequency patterns of the temporal sequences. The key idea of the SFM is to decompose the memory states into different frequency states. In doing so, they can explicitly learn the dependencies of both the low and high frequency patterns. As we will see (cf. Sect. 5.1), RNNs in general can easily learn time series that have a constant frequency spectrum which may be obtained also by Fourier analysis.

[Ollivier et al. \(2015\)](#) suggested to use the “NoBackTrack” algorithm in RNNs to train its parameters. This algorithm works in an online, memoryless setting, which therefore requires no backpropagation through time. It is also scalable, thus avoiding the large computational and memory cost of maintaining the full gradient of the current state with respect to the parameters, but it still uses an iterative method (namely gradient descent). In contrast to this and other related works, in this paper we present a method working with linearly activated RNNs that does not require backpropagation or similar procedures in the learning phase.

3. Predictive Neural Networks

RNNs often host several types of neurons, each activated in a different manner ([Elman, 1990](#); [Hochreiter & Schmidhuber, 1997](#)). In contrast to this, we here simply understand an interconnected group of standard neurons as a neural network which may have arbitrary loops, akin to biological neuronal networks. We adopt a *discrete time model*, i.e., input and output can be represented by a time series and is processed stepwise by the network.

Definition 1 (time series). A *time series* is a series of data points in d dimensions $S(0), \dots, S(n) \in \mathbb{R}^d$ where $d \geq 1$ and $n \geq 0$.

Definition 2 (recurrent neural network). A *recurrent neural network* (RNN) is a directed graph consisting of altogether N nodes, called *neurons*. The *activation* $x(t)$ of a neuron x depends on a discrete time parameter t . We may distinguish three groups of neurons (cf. Fig. 1):

- *input* neurons (usually without incoming edges) whose activation is given by an external source, e.g., a time series,
- *output* neurons (usually without outgoing edges) whose activation represents some output function, and
- *reservoir* or *hidden* neurons (arbitrarily connected) that are used for auxiliary computations.

The edges of the graph represent the network connections. They are usually annotated with *weights* which are compiled in the *transition matrix* W . An entry w_{ij} in row i and column j denotes the weight of the edge from neuron j to neuron i . If there is no connection, then $w_{ij} = 0$. The transition matrix has the form

$$W = \begin{bmatrix} W^{\text{out}} \\ W^{\text{in}} & W^{\text{res}} \end{bmatrix}$$

containing the following weight matrices:

- input weights W^{in} (weights from the input and possibly the output to the reservoir),
- reservoir weights W^{res} (matrix of size $N^{\text{res}} \times N^{\text{res}}$ where N^{res} is the number of reservoir neurons), and
- output weights W^{out} (all weights to the output and possibly back to the input).

Let us now define the *network activity* in more detail: The initial configuration of the neural network is given by a column vector x_0 with N components, called *start vector*. It represents the network state at the start time $t = t_0$. Because of the discrete time model we compute the activation of any

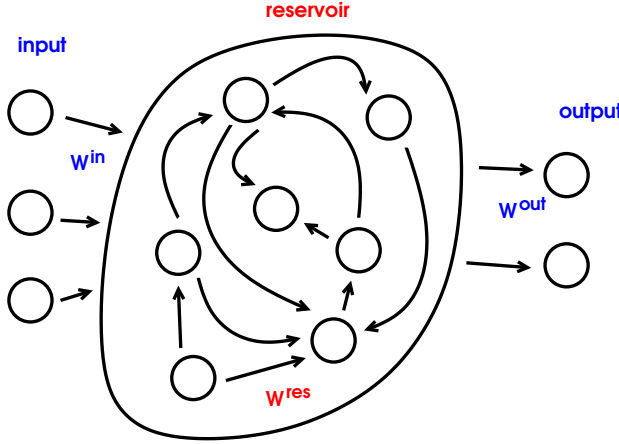


Figure 1. Recurrent neural network (cf. Jaeger, 2007, Fig. 1).

(non-input) neuron y at time $t + \tau$ (for some time step $\tau > 0$) from the activation of the neurons x_1, \dots, x_n , connected to y with the weights w_1, \dots, w_n , at time t , as follows:

$$y(t + \tau) = g(w_1 \cdot x_1(t) + \dots + w_n \cdot x_n(t))$$

This has to be done simultaneously for all neurons of the network. In this context, g is a (real-valued) *activation function*. Usually, a nonlinear, bounded, strictly increasing sigmoidal function g is used, e.g., the logistic function, the hyperbolic tangent (tanh), or the softmax function (cf. Goodfellow et al., 2016). In the following, we employ simply the (linear) identity function and can still approximate arbitrary time-dependent functions (cf. Prop. 3).

Definition 3 (predictive neural network). A *predictive neural network* (PrNN) is a RNN with the following properties:

1. For the start time, it holds $t_0 = 0$, and τ is constant, often $\tau = 1$.
2. The initial input state $S(0)$ of a time series constitutes the first d components of the start vector x_0 .
3. For all neurons we have *linear activation*, i.e., everywhere g is the identity.
4. The weights in W^{in} and W^{res} are initially taken randomly, independently, and identically distributed from the standard normal distribution, whereas the output weights W^{out} are learned (see Sect. 4.1).
5. There is no clear distinction of input and output but only one joint group of d input/output neurons. They may be arbitrarily connected like the reservoir neurons.

PrNNs can run in one of two *modes*: either receiving input or generating (i.e., predicting) output, but not both. Nevertheless, this does not mean that in input receiving mode

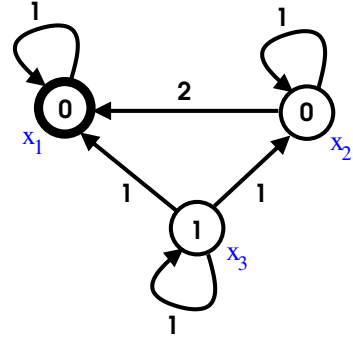


Figure 2. PrNN for $f(t) = t^2$ where $\tau = 1$. The input/output neuron x_1 is marked by a thick border. The initial values of the neurons at time $t_0 = 0$ are written in the nodes. The weights are annotated at the edges.

the output cannot be read off. But since input and output are identical for PrNNs (see above), it is clearly not interesting to read off the just received input as output. We can imagine the whole network as a big reservoir, because the input/output neurons are not particularly special in this case.

Example 1. The function $f(t) = t^2$ can be realized by a PrNN (in output generating mode) with three neurons (see Fig. 2). It exploits the identity $f(t + 1) = t^2 + 2t + 1$. The corresponding transition matrix W and start vector x_0 are:

$$W = \begin{bmatrix} 1 & 2 & 1 \\ 0 & 1 & 1 \\ 0 & 0 & 1 \end{bmatrix} \text{ and } x_0 = \begin{bmatrix} 0 \\ 0 \\ 1 \end{bmatrix}$$

3.1. Network Dynamics

Clearly, a PrNN runs through network states $f(t)$ for $t \geq 0$. It holds (in output generating mode)

$$f(t) = \begin{cases} x_0, & t = 0 \\ W \cdot f(t-1), & \text{otherwise} \end{cases}$$

and hence simply $f(t) = W^t \cdot x_0$.

If the transition matrix W has an eigendecomposition, i.e., there are N distinct eigenvectors, then the networks dynamics can be nicely described by means of the eigenvalues and eigenvectors of W :

Property 1. Let $W = V \cdot D \cdot V^{-1}$ be the eigendecomposition of the transition matrix W with column eigenvectors v_1, \dots, v_N in V and eigenvalues $\lambda_1, \dots, \lambda_N$, on the diagonal of the diagonal matrix D , sorted in decreasing order with respect to their absolute values. Like every column vector, we can represent the start vector x_0 as linear combination of the eigenvectors, namely as $x_0 = x_1 v_1 + \dots + x_N v_N = V \cdot x$ where $x = [x_1 \dots x_N]^\top$. It follows $x = V^{-1} \cdot x_0$. Since W is a linear mapping and for each eigenvector v_k with eigenvalue λ_k with $1 \leq k \leq N$ it holds $W \cdot v_k = \lambda_k v_k$, we have

$W \cdot x_0 = W \cdot (x_1 v_1 + \dots + x_N v_N) = x_1 \lambda_1 v_1 + \dots + x_N \lambda_N v_N$. Induction over t yields immediately:

$$f(t) = W^t \cdot x_0 = x_1 \lambda_1^t v_1 + \dots + x_N \lambda_N^t v_N = V \cdot D^t \cdot x \quad (1)$$

An even more general procedure is to use the *Jordan block decomposition* of the square matrix W . It always exists for algebraic closed fields like the complex numbers. There is also a completely real-valued variant of this normal form (Hogben, 2013). But this special decomposition is needed only if there are less than N distinct eigenvectors (i.e., not all eigenvalues are semisimple). Since this rarely happens, we neglect this case in the following.

So far, the input weights W^{in} and reservoir weights W^{res} are arbitrary random values. In order to obtain better numerical stability during the computation, they should be adjusted as follows:

- In the presence of linear activation, the spectral radius of the reservoir weights matrix W^{res} , i.e., the largest absolute value of its eigenvalues, is set to 1 (cf. Jaeger, 2007). Otherwise, with increasing t , the values of W^t explode, if the spectral radius is greater, or vanish, if the spectral radius is lower.
- The norms of the vectors in W^{in} and W^{res} should be balanced (Koryakin et al., 2012). To achieve this, we initialize the reservoir neurons such that the reservoir start vector r (with N^{res} components; it is part of the start vector x_0) has unit norm by setting:

$$r = \frac{1}{\sqrt{N^{\text{res}}}} \cdot [1 \cdots 1]^{\top}$$

- We usually employ fully connected graphs, i.e., all, especially the reservoir neurons are connected with each other, because the connectivity has nearly no influence on the best reachable performance (Koryakin et al., 2012).

Let us remark that, although the parameter t in Prop. 1 is an integer number, the values of $f(t) = W^t \cdot x_0$ can also be computed for general values of $t \in \mathbb{R}$. For this, since W is diagonalized by the eigendecomposition, we simply have to take the t -th power of each diagonal element in D . Note that, however, the interpolated values of $f(t)$ may be complex, even if W and x_0 are completely real-valued.

3.2. Long-Term Behavior

Let us now investigate the long-term behavior of a RNN (run in output generating mode) by understanding it as an (autonomous) *dynamic system* (Colonius & Kliemann, 2014).

Property 2. Consider an RNN whose transition matrix W is completely real-valued, has an eigendecomposition $W = V \cdot D \cdot V^{-1}$ with a spectral radius 1, and all eigenvalues are distinct, e.g., a pure reservoir. Then, almost all terms $x_k \lambda_k^t v_k$ in Eq. 1 vanish for large t , because for all eigenvalues λ_k with $|\lambda_k| < 1$ we have $\lim_{t \rightarrow \infty} \lambda_k^t = 0$. For the only remaining eigenvalues λ_1 and possibly λ_2 with absolute values 1, we have one of the following cases:

1. $\lambda_1 = +1$. In this case, the network activity contracts to one point, i.e., to a *singularity*: $\lim_{t \rightarrow \infty} W^t \cdot x = x_1 v_1$
2. $\lambda_1 = -1$. For large t it holds $f(t) \approx x_1 (-1)^n v_1$. This means we have an *oscillation* in this case. The dynamic system alternates between two points: $\pm x_1 v_1$
3. λ_1 and λ_2 are two (properly) complex eigenvalues with absolute value 1. Since W is a real-valued matrix, the two eigenvalues as well as the corresponding eigenvectors v_1 and v_2 are complex conjugate with respect to each other. Thus for large t we have an *ellipse* trajectory

$$W^t \cdot x \approx x_1 \lambda_1^t v_1 + x_2 \lambda_2^t v_2 = \tilde{V} \cdot \tilde{D}^t \cdot \tilde{x}$$

where $\tilde{V} = [v_1 \ v_2]$, $\tilde{D} = \begin{bmatrix} \lambda_1 & 0 \\ 0 & \lambda_2 \end{bmatrix}$, and $\tilde{x} = \begin{bmatrix} x_1 \\ x_2 \end{bmatrix}$.

We consider now the latter case in more detail: In this case, the matrix \tilde{V} consists of the two complex conjugated eigenvectors $v = v_1$ and $\bar{v} = v_2$. From all linear combinations of both eigenvectors $\ell(\kappa) = \kappa v + \bar{\kappa} \bar{v}$ for $\kappa \in \mathbb{C}$ with $|\kappa| = 1$, we can determine the vectors with extremal lengths. Since we only have two real-valued dimensions, because clearly the activity induced by the real-valued matrix W remains in the real-valued space, there are two such vectors.

Let now $\kappa = e^{i\varphi} = \cos(\varphi) + i \sin(\varphi)$ (Euler's formula) and $v_{\mathfrak{R}}$ and $v_{\mathfrak{I}}$ be the real and imaginary parts of v , respectively, i.e., $v = v_{\mathfrak{R}} + iv_{\mathfrak{I}}$ and $\bar{v} = v_{\mathfrak{R}} - iv_{\mathfrak{I}}$. Then, for the square of the vector length, it holds:

$$\begin{aligned} \|\ell(\kappa)\|^2 &= \kappa^2 v^2 + 2\kappa \bar{\kappa} v \cdot \bar{v} + \bar{\kappa}^2 \bar{v}^2 = e^{i2\varphi} v^2 + 2v\bar{v} + e^{-i2\varphi} \bar{v}^2 \\ &= 2(\cos(2\varphi)(v_{\mathfrak{R}}^2 - v_{\mathfrak{I}}^2) + (v_{\mathfrak{R}}^2 + v_{\mathfrak{I}}^2) - \sin(2\varphi)(2v_{\mathfrak{R}} \cdot v_{\mathfrak{I}})) \end{aligned}$$

To find out the angle φ with extremal vector length of $\ell(\kappa)$, we have to investigate the derivative of the latter term with respect to φ and compute its zeros. This yields $2(-2\sin(2\varphi)(v_{\mathfrak{R}}^2 - v_{\mathfrak{I}}^2) - 2\cos(2\varphi)(2v_{\mathfrak{R}} \cdot v_{\mathfrak{I}})) = 0$ and thus:

$$\tan(2\varphi) = \frac{-2v_{\mathfrak{R}} \cdot v_{\mathfrak{I}}}{v_{\mathfrak{R}}^2 - v_{\mathfrak{I}}^2}$$

Because of the periodicity of the tangent function there are two main solutions for κ that are orthogonal to each other: $\kappa_1 = e^{i\varphi}$ and $\kappa_2 = e^{i(\varphi + \pi/2)}$. They represent the main axes of an ellipse. All points the dynamic system runs

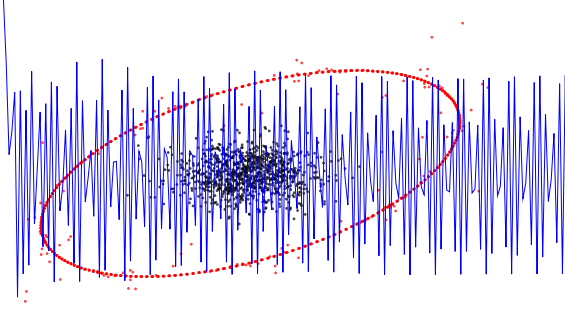


Figure 3. Dynamic system behavior in two dimensions: In the long run, we get an ellipse trajectory (red), though the original data may look like random (black). Projected to one dimension, we have pure sinusoids with one single angular frequency, sampled in large steps (blue).

through in the long run lie on this ellipse. The length ratio of the ellipse axes is $\mu = \|\ell(\kappa_1)\| / \|\ell(\kappa_2)\|$. We normalize both vectors to unit length and put them in the matrix $\hat{V} = [\ell(\kappa_1) / \|\ell(\kappa_1)\| \quad \ell(\kappa_2) / \|\ell(\kappa_2)\|]$.

We now build a matrix \hat{D} , similar to \tilde{D} but completely real-valued, which states the ellipse rotation. The rotation speed can be derived from the eigenvalue $\lambda = \lambda_1$. In each step of length τ , there is a rotation by the angle $\rho\tau$, which can be determined from the equation $\lambda = |\lambda|(\cos(\rho\tau) + i\sin(\rho\tau))$. The two-dimensional ellipse trajectory can be stated by two (co)sinusoids: $f(t) = [a \cos(\rho t) \quad b \sin(\rho t)]^\top$ with $a, b > 0$. Applying the addition theorems of trigonometry, we get:

$$\begin{aligned} f(t + \tau) &= \begin{bmatrix} a \cos(\rho(t + \tau)) \\ b \sin(\rho(t + \tau)) \end{bmatrix} \\ &= \begin{bmatrix} a(\cos(\rho t) \cos(\rho \tau) - \sin(\rho t) \sin(\rho \tau)) \\ b(\sin(\rho t) \cos(\rho \tau) + \cos(\rho t) \sin(\rho \tau)) \end{bmatrix} \\ &= \underbrace{\begin{bmatrix} \cos(\rho \tau) & -a/b \sin(\rho \tau) \\ b/a \sin(\rho \tau) & \cos(\rho \tau) \end{bmatrix}}_{\hat{D}} \cdot f(t) \end{aligned}$$

From this, we can read off the desired ellipse rotation matrix \hat{D} as indicated above and $\mu = a/b$. Finally, we can determine the corresponding two-dimensional start vector \hat{x} by solving the equation $\hat{V} \cdot \hat{D} \cdot \hat{x} = \tilde{V} \cdot \tilde{D} \cdot \tilde{x}$.

In summary, we have $W^t \cdot x_0 \approx \hat{V} \cdot \hat{D}^t \cdot \hat{x}$ for large t . Every RNN with many neurons can thus be approximated by a simple network with at most two neurons, defined by the matrix \hat{D} and start vector \hat{x} . The output values can be computed for all original dimensions by multiplication with the matrix \hat{V} . They lie on an ellipse in general. Nonetheless, in the beginning, i.e., for small t , the dynamics of the system is not that regular (cf. Fig. 3).

The long-term behavior of PrNNs is related to that of ESNs. For the latter, usually the activation function is \tanh and the spectral radius is smaller than 1. Then reservoirs with zero input collapse because of $|\tanh(z)| \leq z$ for all $z \in \mathbb{R}$ but the convergence may be rather slow. This leads to the so-called *echo state property* (Manjunath & Jaeger, 2013): Any random initial state of a reservoir is forgotten, such that after a washout period the current network state is a function of the driving input. In contrast to ESNs, PrNNs have linear activation and usually a spectral radius of 1 (cf. Def. 3). But as we have just shown, there is a similar effect in the long run: The network activity reduces to at most two dimensions which are independent from the initial state of the network.

3.3. Real-Valued Transition Matrix Decomposition

For real-valued transition matrices W , it is possible to define a decomposition that, in contrast to the eigendecomposition from Prop. 1, solely makes use of real-valued components. For this, we transform the matrices V and D from the eigen-decomposition, applying the insights from Sect. 3.2. The transformed matrices, called V' and D' henceforth, are obtained by the following procedure:

- Every real-valued eigenvalue λ and corresponding eigenvector v remain in D and V , respectively, as is.
- For each complex conjugated eigenvalue pair λ and $\bar{\lambda}$, the respective submatrix \tilde{D} in D is replaced by \hat{D} multiplied by $|\lambda| = |\bar{\lambda}|$. The corresponding two eigenvectors in V are replaced by the vectors in \hat{V} .

Analogously to Prop. 1, for the real-valued decomposition of the transition matrix W it holds

$$W^t \cdot x_0 = V' \cdot D'^t \cdot x'$$

where $x' = V'^{-1} \cdot x_0$. Note that x' contains \hat{x} in two subsequent components. This observation incidentally allows an alternative way to compute \hat{x} (cf. Sect. 3.2).

4. Learning Predictive Neural Networks

Functions can be learned and approximated by PrNNs in two steps: First, as for ESNs (Jaeger, 2007), we only learn the output weights W^{out} ; all other connections remain unchanged. Second, if possible, we reduce the network size; this often leads to better generalization and avoids overfitting. Thus, in contrast to many other approaches, the network architecture is changed during the learning process.

4.1. Learning the Output Weights

To learn the output weights W^{out} , we run the input values from the time series $S(0), \dots, S(n)$ through the network (in

input receiving mode), particularly through the reservoir. For this, we build the sequence of corresponding reservoir states $R(0), \dots, R(n)$:

$$R(t_0) = r \text{ and } R(t + \tau) = \begin{bmatrix} W^{\text{in}} & W^{\text{res}} \end{bmatrix} \cdot \begin{bmatrix} S(t) \\ R(t) \end{bmatrix}$$

We want to predict the next input value $S(t + \tau)$, given the current input and reservoir states $S(t)$ and $R(t)$. To achieve this, we comprise all but the last input and reservoir states in one matrix X with:

$$X = \begin{bmatrix} S(0) & \dots & S(n-1) \\ R(0) & \dots & R(n-1) \end{bmatrix}$$

Each output value corresponds to the respective next input value $S(t + \tau)$. For this, we compose another matrix $Y^{\text{out}} = [S(1) \dots S(n)]$ where the first value $S(0)$ clearly has to be omitted. We compute $Y^{\text{out}}(t) = S(t + \tau)$ from $X(t)$ by assuming a linear dependency:

$$Y^{\text{out}} = W^{\text{out}} \cdot X \quad (2)$$

Its solution can easily be determined as $W^{\text{out}} = Y^{\text{out}}/X$, where $/$ denotes the operation of solving a linear equation system, possibly applying the least squares method in case of an overdetermined system, as implemented in scientific programming languages like Octave (Eaton et al., 2017) or Matlab (Higham & Higham, 2017).

Prediction of further values is now possible (in output generating mode) as follows:

$$\begin{bmatrix} S(t + \tau) \\ R(t + \tau) \end{bmatrix} = W \cdot \begin{bmatrix} S(t) \\ R(t) \end{bmatrix} \text{ with } W \text{ as in Def. 2}$$

This first phase of the learning procedure is related to a linear autoregressive model (Akaike, 1969). It specifies that the output depends linearly on its own previous values and on a stochastic term (white noise). In consequence the model is in the form of a stochastic difference equation as in general (physical) dynamic systems (Colonius & Kliemann, 2014). However, one important difference to a simple autoregressive model is that for PrNNs the output does not only depend on its own previous values and possibly white noise but on the complete state of the possibly big reservoir whose dynamics is explicitly dealt with in the reservoir matrix W^{res} .

4.2. An Approximation Theorem

Property 3. From a function $f(t)$ in $d \geq 1$ dimensions, let a series of function values $f(t_0), \dots, f(t_n)$ be given. Then there is a PrNN with the following properties:

1. It runs exactly through all given $n + 1$ function values, i.e., it approximates $f(t)$.

2. It can effectively be learned by the above-stated solution procedure (Sect. 4.1).

To see this, we take the series of function values $f(t_0), \dots, f(t_n)$ and identify them with the time series $S(0), \dots, S(n)$. The procedure for learning output weights (cf. Sect. 4.1) uses the reservoir state sequence as part of the coefficient matrix X which reduces to at most two dimensions however – independent of the number of reservoir neurons (cf. Sect. 3.2). Therefore the rank of the coefficient matrix X is not maximal in general and thus the linear equation system from Eq. 2 often has no solutions (although we may have an equation system with the same number of equations and unknowns). A simple increase of the number of reservoir neurons does not help much.

A system of linear equations has at least one solution if and only if the rank of the coefficient matrix X is equal to the rank of its augmented matrix. To achieve this, we do not learn only the output weights as in ESNs (Jaeger, 2007) but the complete transition matrix W , starting with a random reservoir state sequence matrix $[R(0) \dots R(n)]$ for sufficiently many reservoir neurons which is considered as additional input in this case. If all elements of this matrix are taken independently and identically distributed from the standard normal distribution, its rank is almost always maximal. Let d' be the rank of the matrix $[S(0) \dots S(n-1)]$ and:

$$Y = \begin{bmatrix} S(1) & \dots & S(n) \\ R(1) & \dots & R(n) \end{bmatrix}$$

Then the linear matrix equation $W \cdot X = Y$ almost always has at least one solution, if $N^{\text{res}} \geq n - d'$ reservoir neurons are employed.

The just sketched proof of Prop. 3 suggests a way to learn the input and reservoir weights. This topic is also investigated by Palangi et al. (2013) for ESNs with nonlinear activation function in the reservoir. However, for PrNNs, the given input and reservoir weights W^{in} and W^{res} together with the learned output weights W^{out} provide the best approximation of the function $f(t)$. There is no need to learn them, because PrNNs are completely linearly activated RNNs (including the reservoir). If one tries to learn W^{in} and W^{res} taking not only the output time series S but additionally the reservoir state time series R into account, then in principle exactly the given input and reservoir weights are learned. Nonetheless, W^{in} and W^{res} can be learned as sketched above by our procedure, if they are not given in advance, starting with a random reservoir state sequence. But our experiments indicate that this procedure is numerically more unstable than the one with given input and reservoir weights (as described in Sect. 4.1).

Prop. 3 is related to the *universal approximation theorem* for feedforward neural networks (Hornik, 1991). It states

that a (non-recurrent) network with a linear output layer and at least one hidden layer activated by a nonlinear, sigmoidal function can approximate any continuous function on a closed and bounded subset of the \mathbb{R}^n from one finite-dimensional space to another with any desired non-zero amount of error, provided that the network is given enough hidden neurons (Goodfellow et al., 2016). Since RNNs are more general than feedforward networks, the universal approximation theorem also holds for them (see also Maass et al., 2002).

In contrast to the universal approximation theorem, for Prop. 3 linearly activated neurons suffice, but the approximated function has only one-dimensional input, namely t . Another difference between PrNNs and nonlinearly activated feedforward neural networks is that the former can learn the function $f(t)$ efficiently. No iterative method like backpropagation is required; we just have to solve a linear equation system. Thus learning is as easy as learning a single-layer perceptron, which however is restricted in expressibility because only linearly separable functions can be represented.

4.3. Network Reduction

To approximate a function exactly for sure, we need a high number N^{res} of reservoir neurons in Prop. 3. It is certainly a good idea to lower this number. We can do this by simply taking a smaller number of reservoir neurons. Nonetheless, besides that, we may (and will) reduce the dimensionality of the transition matrix W in a more controlled way – after learning the output weights.

For ESNs, dimensionality reduction is considered, too, namely by means of so-called *conceptors* (Jaeger, 2014). These are special matrices which restrict the reservoir dynamics to a linear subspace characteristic for a specific pattern. However, as in principal component analysis, conceptors reduce only the spatial dimensionality of the point cloud of the given data. In contrast to this, in what follows, we reduce the transition matrix and hence take also into account the temporal order of the data points in the time series.

Property 4. Let W be the transition matrix of a PrNN that approximates the given function with high accuracy. For the moment, let us focus on the case of $d = 1$ output dimensions. Then it holds $f(t) = \alpha_1 \lambda_1^t + \dots + \alpha_N \lambda_N^t$ for the output, where $\alpha_1, \dots, \alpha_N \in \mathbb{C}$ can be determined from Prop. 1 and $\lambda_1, \dots, \lambda_N$ are the eigenvalues of W . For n training examples (corresponding to the number of linear equations), the k -th network component can be omitted, if the squared absolute

error sum

$$E_k = \sum_{t=1}^n |\alpha_k \lambda_k^t|^2 = \begin{cases} \frac{|\alpha_k \lambda_k|^2 (1 - |\lambda_k|^{2n})}{1 - |\lambda_k|^2}, & \text{for } |\lambda_k| \neq 1 \\ n \cdot |\alpha_k|^2, & \text{otherwise} \end{cases}$$

is small enough.

Roughly speaking, the latter holds if $|\alpha_k| \approx 0$ and/or $|\lambda_k| \ll 1$. In practice, we take all network components k with the largest values of E_k as long as their cumulated sum is below a given threshold $\theta \leq 1$ for the desired precision which can be defined as fraction of $\sum_{k=1}^N E_k$.

In general, we call a network component k *relevant* if it is taken in the procedure above for at least one of the $d \geq 1$ input/output components. From V and D , and x (according to Prop. 1), we derive now reduced matrices \hat{V} and \hat{D} , and the vector \hat{x} as follows:

- From V , take the rows corresponding to the input/output components and the columns corresponding to the relevant network components.
- From D , take the rows and columns corresponding to the relevant network components.
- From x , take the rows corresponding to the relevant network components.

If W is real-valued, \hat{V} , \hat{D} , and \hat{x} should be real-valued, too. To achieve this, we take the relevant components from V' , D' , and x' instead of V , D , and x . In this case, however, we always have to treat pairs of complex conjugated eigenvalues λ_k and $\overline{\lambda_k}$ simultaneously, together with the corresponding coefficients α_k and $\overline{\alpha_k}$. The squared absolute error sum (which should be normalized to one component by dividing it with 2^2) for the whole pair in one output dimension is:

$$\begin{aligned} \sum_{t=1}^n |\alpha_k \lambda_k^t + \overline{\alpha_k} \overline{\lambda_k}^t|^2 &= \frac{(\alpha_k \lambda_k)^2 (1 - \lambda_k^{2n})}{1 - \lambda_k^2} \\ &+ 2 \frac{|\alpha_k \lambda_k|^2 (1 - |\lambda_k|^{2n})}{1 - |\lambda_k|^2} + \frac{\overline{\alpha_k} \overline{\lambda_k}^2 (1 - \overline{\lambda_k}^{2n})}{1 - \overline{\lambda_k}^2} \\ &= 2 \left(\Re \left(\frac{(\alpha_k \lambda_k)^2 (1 - \lambda_k^{2n})}{1 - \lambda_k^2} \right) + E_k \right) \end{aligned}$$

In the latter formula, \Re denotes the real part of the respective complex value. The equality holds, because conjugation is a field automorphism, hence compatible with $+$ and \cdot , and $z + \bar{z} = 2 \Re(z)$ for all $z \in \mathbb{C}$.

Eventually, we arrive at another approximation formula:

$$f(t) \approx \hat{V} \cdot \hat{D}^t \cdot \hat{x}$$

The corresponding network has the start vector \hat{x} , a reservoir with the transition matrix \hat{D} , and output weights given by the matrix \hat{V} . Because of the separate output weights, actually the value for $f(t)$ is obtained one time step too late, but this can be repaired simply by starting with $\hat{D}^{-1} \cdot \hat{x}$ instead of \hat{x} .

Note that the dimensionality reduction does not only lead to a smaller number of reservoir neurons, but also to a rather simple network structure: The transition matrix \hat{D} (which comprises the reservoir weights W^{res} of the reduced network) is a sparse matrix with non-zero elements only on the main and immediately neighbored diagonals. Thus the number of connections is in $O(N)$, i.e., linear in the number of reservoir neurons, not quadratic – as in general.

Our procedure of dimensionality reduction obviously leads to a new network architecture. However, in contrast to other approaches, we do not learn the new network architecture by incremental derivation from the original network, but in only one step exploiting the eigendecomposition of the transition matrix. From this, we obtain small, efficient, and sparsely connected networks, as we have just seen.

4.4. Complexity and Generalization of the Procedure

Property 5. In both learning steps, it is possible to employ any of the many available fast and constructive algorithms for linear regression and eigendecomposition. Therefore, the time complexity is just $O(N^3)$ for both output weights learning and dimensionality reduction (cf. Demmel et al., 2007). In theory, if we assume that the basic numerical operations like $+$ and \cdot can be done in constant time, the asymptotic complexity is even a bit better. In practice, however, the complexity depends on the bit length of numbers in floating point arithmetics, of course, and may be worse hence. The size of the learned network is in $O(N)$ (cf. Sect. 4.3).

Note that feedforward networks with three threshold neurons already are NP-hard to train (cf. Blum & Rivest, 1992). This results from the fact that the universal approximation theorem for feedforward networks differs from Prop. 3, because the former holds for multi-dimensional functions and not only time-dependent input. In this light, the computational complexity of $O(N^3)$ for PrNNs does not look overly expensive. Furthermore, it is the overall time complexity of the whole learning procedure, because it is not embedded in a time-consuming iterative learning procedure (like backpropagation) as in other state-of-the-art methods.

We observe that most of the results presented in this paper still hold, if the transition matrix W contains complex numbers. This means in particular that also complex functions can be learned (from complex-valued time series) and represented by predictive neural networks (Prop. 3). The procedure for treating the error of complex conjugated eigenvalue pairs (cf. Sect. 4.3) becomes superfluous then. Nonetheless,

the long-term behavior of networks with a random complex transition matrix W differs from the one described in Sect. 3.2, because then usually there are no pairs of complex conjugated eigenvalues with absolute values 1.

5. Experiments

In this section, we demonstrate the evaluation results for PrNNs on several tasks of learning and predicting time series and approximate them by a function $f(t)$ represented by a RNN. We consider the following benchmarks: multiple superimposed oscillators, number puzzles, and robot soccer simulation. All experiments are performed with a program written by the authors in Octave (Eaton et al., 2017) that implements the PrNN learning procedure (cf. Sect. 4). Let us start with an example that illustrates the overall method.

Example 2. The graphs of the functions $f_1(t) = 4t(1-t)$ (parabola) and $f_2(t) = \sin(\pi t)$ (sinusoid) look rather similar for $t \in [0, 1]$, see Fig. 4. Can both functions be learned and distinguished from each other?

To investigate this, we sample both graphs for $t \in [0, 1]$ with $\tau = 0.01$. After that, we learn the output weights W^{out} (cf. Sect. 4.1), starting with a large enough reservoir consisting of up to $N^{\text{res}} = 100$ neurons (cf. Prop. 3). Finally, we reduce the size of the overall transition matrix W with precision threshold $\theta = 0.99$ (cf. Sect. 4.3). Minimal PrNNs consist of $N_1 = 3$ neurons for the parabola (cf. Ex. 1) and $N_2 = 2$ neurons for the sinusoid (cf. Sect. 3.2). They are learned already with $N^{\text{res}} = 30$ reservoir neurons in the beginning in about 65% (parabola) or even 100% (sinusoid) of the trials, see also Fig. 5. Learning the parabola is more difficult because the corresponding transition matrix W (cf. Ex. 1) has no proper eigendecomposition. The root mean square error normalized to the number of all sample components (called NRMSE henceforth) is only about 10^{-6} in both cases.

5.1. Multiple Superimposed Oscillators

Multiple superimposed oscillators (MSO) count as difficult benchmark problems for RNNs (cf. Koryakin et al., 2012; Schmidhuber et al., 2007; Xue et al., 2007). The corresponding time series is generated by summing up several simple sinusoids. Formally it is described by

$$S(t) = \sum_{k=1}^n \sin(\alpha_k t)$$

where $n \leq 8$ denotes the number of sinusoids and $\alpha_k \in \{0.2, 0.311, 0.42, 0.51, 0.63, 0.74, 0.85, 0.97\}$ their frequencies. Various publications have investigated the MSO problem with different numbers of sinusoids. We concentrate here solely on the case $n = 8$ whose graph is shown in Fig. 6, because in contrast to other approaches it is still easy to learn for PrNNs.

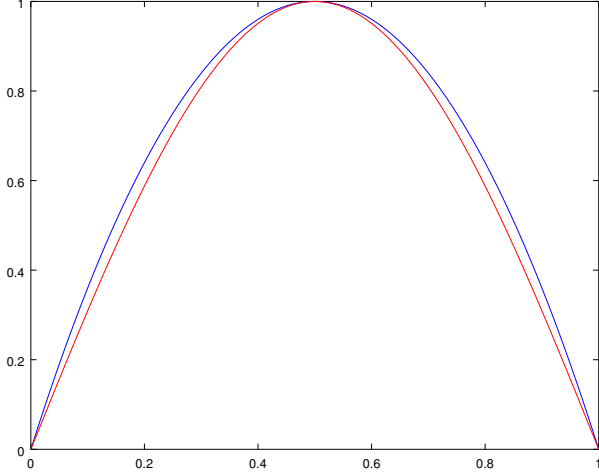


Figure 4. Ex. 2: Parabola or sinusoid – that is the question.

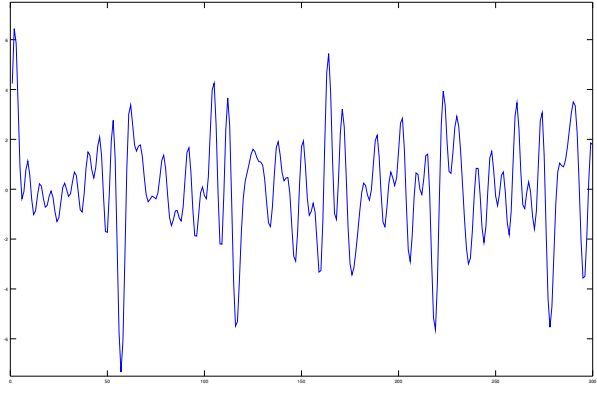


Figure 6. The signal of eight multiple superimposed oscillators (for $1 \leq t \leq 300$) does not have a simple periodic structure. PrNN learning leads to minimal networks with only $N = 16$ reservoir neurons, i.e., two for each frequency in the signal.

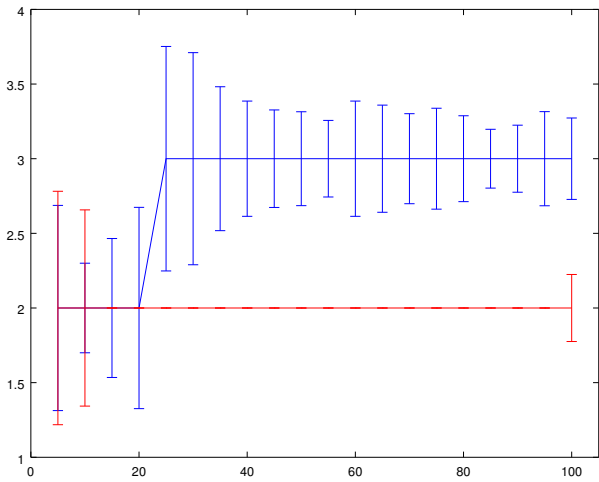


Figure 5. The error bar diagram shows the reduced versus the initial number of reservoir neurons for Ex. 2 (median of 100 trials). It demonstrates that by PrNN learning the number of reservoir neurons can be reduced to only $N_1 = 3$ (parabola, blue) or $N_2 = 2$ (sinusoid, red), respectively. In both cases, the neural networks have minimal size.

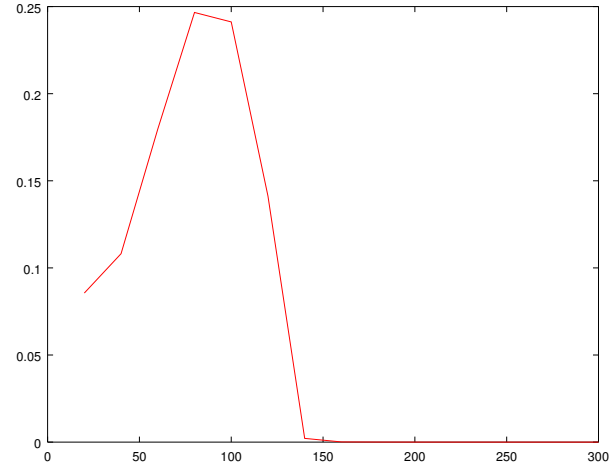


Figure 7. The diagram shows the NRMSE (median of 100 trials) versus the initial number N^{res} of reservoir neurons for the MSO example. The NRMSE is rather small (about 10^{-3}), if we start with about $N^{\text{res}} \geq 140$ reservoir neurons.

Applying the PrNN learning procedure again with $\theta = 0.99$ and taking as many time steps as reservoir neurons, we arrive at PrNNs with only $N = 16$ reservoir neurons in most cases. Since two neurons are required for each frequency (cf. Sect. 3.2), this is the minimal size. Furthermore, if we start with a large enough reservoir, the NRMSE is rather small (see Fig. 7). Thus PrNNs outperform the previous state-of-the-art for the MSO task with a minimal number of units. Koryakin et al. (2012) report $N^{\text{res}} = 68$ as the optimal reservoir size for ESNs, but in contrast to our approach, this number is not further reduced. In general a PrNN with $2n$ neurons suffices to represent a signal, which might be a musical harmony (cf. Stolzenburg, 2017), consisting of n sinusoids. It can be learned by the PrNN learning procedure with dimension reduction (see also Neitzel, 2018).

5.2. Solving Number Puzzles

Example 3. Number series tests are a popular task in intelligence tests. The function represented by a number series can be learned by artificial neural networks, in particular RNNs. Glüge & Wendemuth (2013) list 20 number puzzles (cf. Ragni & Klein, 2011), among them are the series:

$$\begin{aligned} S_8 &= [28, 33, 31, 36, 34, 39, 37, 42] \quad f(t) = f(t-2) + 3 \\ S_9 &= [3, 6, 12, 24, 48, 96, 192, 384] \quad f(t) = 2f(t-1) \\ S_{15} &= [6, 9, 18, 21, 42, 45, 90, 93] \\ &\quad f(t) = 2f(t-2) + 4.5 + 1.5(-1)^{t-1} \\ S_{19} &= [8, 12, 16, 20, 24, 28, 32, 36] \quad f(t) = f(t-1) + 4 \end{aligned}$$

We apply the PrNN learning procedure to all 20 examples taking small reservoirs ($N^{\text{res}} \approx 4$) and do not perform dimensionality reduction because the number series are too short for this. This also leads to more general functions which seems to be appropriate because number puzzles are usually presented to humans. The first 7 of 8 elements of each series is given as input. If the output of the learned network predicts the given input correctly, then the last (8-th) element is predicted (cf. Sect. 4.1).

Tab. 1 lists the percentages of correct predictions of the last element. The most frequently predicted last element (simple majority) is the correct one in most cases, namely 75% for $N^{\text{res}} = 4$. Exceptions are the series S_8 and S_{15} which are the only series with definitions recurring to $f(t-2)$ but not $f(t-1)$. If we always add the previous values of the time series as clue to the input, then the correctness of the procedure can be increased significantly (to 95% for $N^{\text{res}} = 4$).

5.3. Replaying Soccer Games

RoboCup (Kitano et al., 1997) is an international scientific robot competition in which teams of multiple robots compete against each other. Its different leagues provide many sources of robotics data that can be used for further analysis and application of machine learning. A soccer simulation game lasts 10 mins and is divided into 6000 time steps where the length of each cycle is 100 ms. Logfiles contain information about the game, in particular about the current positions of all players and the ball including velocity and orientation for each cycle. Michael et al. (2018) describe a research dataset using some of the released binaries of the RoboCup 2D soccer simulation league (Chen et al., 2003) from 2016 and 2017 (see also Michael et al., 2017). In our experiments we evaluated ten games of the top-five teams (available from <http://oliver.obst.eu/data/RoboCupSimData/overview.html>), considering only the (x, y) -coordinates of the ball and the altogether 22 players for all time points during the so-called “play-on” mode (see also Steckhan, 2018).

series	$N^{\text{res}} = 3$	$N^{\text{res}} = 4$	$N^{\text{res}} = 5$	clue
S_1	37,7%	33,5%	0,7%	22,5%
S_2	28,9%	46,2%	29,2%	18,6%
S_3	46,7%	52,8%	1,4%	45,4%
S_4	23,7%	30,0%	18,0%	40,3%
S_5	57,3%	67,6%	43,1%	66,7%
S_6	33,2%	54,1%	17,1%	64,4%
S_7	59,4%	58,9%	57,5%	51,5%
S_8	20,1%	23,4%	1,7%	32,7%
S_9	100,0%	100,0%	100,0%	100,0%
S_{10}	50,8%	68,4%	69,8%	59,3%
S_{11}	45,4%	63,0%	4,1%	68,1%
S_{12}	13,7%	24,2%	11,3%	37,5%
S_{13}	65,2%	56,4%	43,1%	37,6%
S_{14}	43,2%	63,1%	2,7%	58,0%
S_{15}	3,4%	8,5%	2,6%	3,6%
S_{16}	36,3%	47,2%	3,2%	48,5%
S_{17}	21,5%	28,5%	7,6%	23,3%
S_{18}	34,7%	31,5%	0,9%	23,2%
S_{19}	47,3%	69,8%	73,0%	57,3%
S_{20}	39,1%	39,6%	0,1%	24,2%

Table 1. Percentages of correct predictions of the last element for 20 number puzzles (Ragni & Klein, 2011; Glüge & Wendemuth, 2013) in 1000 trials. In the last case, $N^{\text{res}} = 4$ reservoir neurons are employed and the previous series value is used as a clue.

For PrNN learning, we use only every 10-th time step of each game with $d = 2 + 2 \cdot 22 = 46$ input dimensions and start with a reservoir consisting of $N^{\text{res}} = 500$ neurons. We repeat the learning procedure until the NRMSE is smaller than 1; on average, already two attempts suffice for this. This means, if we replay the game by the learned PrNN (in output generating mode), then on average the predicted positions deviate less than 1 m from the real ones – over the whole length of the game (cf. Fig. 8). Dimensionality reduction leads to a significant reduction of the network size – about 24% if we concentrate on the relevant components for the ball trajectory (cf. Tab. 2). The complete learning procedure runs in seconds on standard hardware.

6. Conclusions

In this paper, we have introduced PrNNs – a simple and yet powerful type of RNNs where all neurons are linearly activated. The learning procedure employs only standard matrix operations and is thus quite fast. No backpropagation, gradient descent, or other iterative procedure is required. In contrast to ESNs, also no washout period is required in the beginning. Any function can be approximated directly from the first step and with an arbitrary starting vector. The major innovation of PrNNs is dimensionality reduction (cf. Sect. 4.3). It means that not only network weights but also the network architecture is learned, leading to significantly

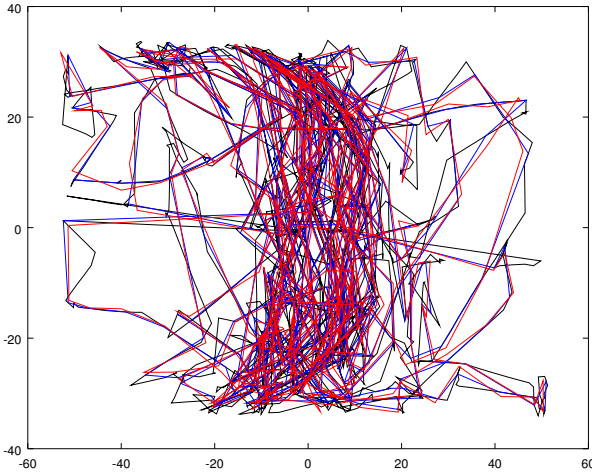


Figure 8. Ball trajectory of robot soccer simulation game #2 (*Gliders* 2016 versus *HELIOS* 2017) on a pitch of size 105 m×68 m. The original trajectory of the ball during play is shown for all time steps (black). The game can be replayed by a PrNN with $N^{\text{res}} = 500$ reservoir neurons with high accuracy (blue). The reduced network with $N^{\text{res}} = 389$ reservoir neurons still mimics the trajectory with only small error (red).

game	NRMSE(1)	NRMSE(2)	net size
#1	0.00013	0.66976	427
#2	0.00534	0.85794	389
#3	0.00048	0.81227	384
#4	0.00006	0.66855	408
#5	0.00002	0.65348	424
#6	0.00000	0.98644	327
#7	0.00000	0.75411	370
#8	0.00008	0.70957	385
#9	0.00000	0.67534	328
#10	0.00017	0.86802	364

Table 2. For ten RoboCup simulation games, a PrNN is learned with initially $N^{\text{res}} = 500$ reservoir neurons. The table shows the NRMSE (1) before and (2) after dimensionality reduction where $\theta = 0.999$. The network size can be reduced significantly – about 24% on average (last column).

smaller and sparsely connected networks.

Although any time-dependent function can be approximated with arbitrary precision (cf. Prop. 3), not any function can be implemented by RNNs, in particular functions increasing faster than single-exponential (cf. Prop. 1) like 2^t (double-exponential) or $t!$ (factorial function). Nevertheless, experiments with reasonably large example and network sizes can be performed successfully within seconds on standard hardware, e.g., with the robot soccer dataset (cf. Sect. 5.3). However, if thousands of reservoir neurons are employed, the procedure may become numerically unstable, at least our Octave implementation. The likelihood of almost identical eigenvectors and eigenvalues with absolute values greater than 1 in the learned transition matrix W is increased then.

Future work shall therefore try to make the procedure even more stable. Like in convolutional networks (cf. Goodfellow et al., 2016), further input can be introduced giving additional clue, which may improve the predictive and memory capacity of PrNNs (cf. Marzen, 2017). Last but not least, other machine learning tasks besides prediction shall be addressed, including classification and reinforcement learning.

Acknowledgements

We would like to thank Andrew Francis, Rouven Neitzel, Oliver Otto, Kai Steckhan, Flora Stolzenburg, and Ruben Zilibowitz for helpful discussions and comments. The research reported in this paper has been supported by the German Academic Exchange Service (DAAD) by funds of the German Federal Ministry of Education and Research (BMBF) in the Programmes for Project-Related Personal Exchange (PPP) under grant no. 57319564 and Universities Australia (UA) in the Australia-Germany Joint Research Cooperation Scheme within the project *Deep Conceptors for Temporal Data Mining* (Decorating).

References

Akaike, Hirotugu. Fitting autoregressive models for prediction. *Annals of the Institute of Statistical Mathematics*, 21(1):243–247, 1969. URL <http://link.springer.com/content/pdf/10.1007/BF02532251.pdf>.

Bengio, Yoshua, Simard, Patrice, and Frasconi, Paolo. Learning long-term dependencies with gradient descent is difficult. *IEEE Transactions on Neural Networks*, 5(2):157–166, 1994. ISSN 1045-9227. URL <http://doi.org/10.1109/72.279181>.

Blum, Avrim L. and Rivest, Ronald L. Training a 3-node neural network is NP-complete. *Neural Networks*, 5(1):117–127, 1992. URL [http://doi.org/10.1016/S0893-6080\(05\)80010-3](http://doi.org/10.1016/S0893-6080(05)80010-3).

Chen, Mao, Dorer, Klaus, Foroughi, Ehsan, Heintz, Fredrick, Huang, ZhanXiang, Kapetanakis, Spiros, Kos- tiadis, Kostas, Kummeneje, Johan, Murray, Jan, Noda, Itsuki, Obst, Oliver, Riley, Pat, Steffens, Timo, Wang, Yi, and Yin, Xiang. *Users Manual: RoboCup Soccer Server – for Soccer Server Version 7.07 and Later*. The RoboCup Federation, February 2003. URL http://helios.hampshire.edu/jdavila/cs278/virtual_worlds/robocup_manual-20030211.pdf.

Colonius, Fritz and Kliemann, Wolfgang. *Dynamical Systems and Linear Algebra*, volume 158 of *Graduate Studies in Mathematics*. American Mathematical Society, Providence, Rhode Island, 2014. URL <http://doi.org/10.1090/gsm/158>.

Demmel, James, Dumitriu, Ioana, and Holtz, Olga. Fast linear algebra is stable. *Numerische Mathematik*, 108(1): 59–91, 2007. ISSN 0945-3245. URL <http://doi.org/10.1007/s00211-007-0114-x>.

Deng, Li and Yu, Dong. Deep learning: Methods and applications. *Foundations and Trends in Signal Processing*, 7(3-4):198–387, 2014. URL <http://research.microsoft.com/pubs/209355/DeepLearning-NowPublishing-Vol17-SIG-039.pdf>.

Eaton, John Wesley, Bateman, David, Hauberg, Søren, and Wehbring, Rik. *GNU Octave – A High-Level Interactive Language for Numerical Computations*, 2017. URL <http://www.octave.org/>. Edition 4 for Octave version 4.2.1.

Elman, Jeffrey L. Finding structure in time. *Cognitive Science*, 14:179–211, 1990. ISSN 0364-0213. URL <http://crl.ucsd.edu/~elman/Papers/fsit.pdf>.

Glüge, Stefan and Wendemuth, Andreas. Solving number series with simple recurrent networks. In de Vicente, José Manuel Ferrández, Sánchez, José Ramón Álvarez, de la Paz López, Félix, and Toledo-Moreo, F. Javier (eds.), *Natural and Artificial Models in Computation and Biology – 5th International Work-Conference on the Interplay Between Natural and Artificial Computation, IWINAC 2013. Proceedings, Part I*, LNCS 7930, pp. 412–420. Springer, 2013. URL http://doi.org/10.1007/978-3-642-38637-4_43.

Goodfellow, Ian, Bengio, Yoshua, and Courville, Aaron. *Deep Learning*. Adaptive Computation and Machine Learning. MIT Press, Cambridge, MA, London, 2016. URL <http://www.deeplearningbook.org>.

Higham, Desmond J. and Higham, Nicholas J. *MatLab Guide*. Siam, Philadelphia, PA, 3rd edition, 2017. URL <http://bookstore.siam.org/ot150/>.

Hochreiter, Sepp and Schmidhuber, Jürgen. Long short- term memory. *Neural Computation*, 9(8):1735–1780, 1997. ISSN 0899-7667. URL <http://doi.org/10.1162/neco.1997.9.8.1735>.

Hogben, Leslie. Canonical forms. In *Handbook of Linear Algebra*, Discrete Mathematics and Its Applications, chapter 6. Chapman and Hall/CRC, Boca Raton, FL, 2nd edition, 2013.

Hornik, Kurt. Approximation capabilities of multilayer feedforward networks. *Neural Networks*, 4(2):251–257, 1991. ISSN 0893-6080. URL [http://doi.org/10.1016/0893-6080\(91\)90009-T](http://doi.org/10.1016/0893-6080(91)90009-T).

Hu, Hao and Qi, Guo-Jun. State-frequency memory recurrent neural networks. In Precup, Doina and Teh, Yee Whye (eds.), *Proceedings of the 34th International Conference on Machine Learning*, volume 70 of *Proceedings of Machine Learning Research*, pp. 1568–1577, International Convention Centre, Sydney, Australia, 2017. PMLR. URL <http://proceedings.mlr.press/v70/hu17c.html>.

Jaeger, Herbert. Echo state network. *Scholarpedia*, 2(9):2330, 2007. URL <http://doi.org/10.4249/scholarpedia.2330>. Revision #151757.

Jaeger, Herbert. Controlling recurrent neural networks by conceptors. CoRR – Computing Research Repository abs/1403.3369, Cornell University Library, 2014. URL <http://arxiv.org/abs/1403.3369>.

Kitano, Hiroaki, Asada, Minoru, Kuniyoshi, Yasuo, Noda, Itsuki, Osawa, Eiichi, and Matsubara, Hitoshi. RoboCup: A challenge problem for AI. *AI Magazine*, 18(1):73–85, 1997.

Koryakin, Danil, Lohmann, Johannes, and Butz, Martin V. Balanced echo state networks. *Neural Networks*, 36:35–45, 2012. ISSN 0893-6080. URL <http://doi.org/10.1016/j.neunet.2012.08.008>.

Lipton, Zachary C., Berkowitz, John, and Elkan, Charles. A critical review of recurrent neural networks for sequence learning. CoRR – Computing Research Repository <http://arxiv.org/abs/1506.00019>, Cornell University Library, 2015.

Maass, Wolfgang, Natschläger, Thomas, and Markram, Henry. Real-time computing without stable states: A new framework for neural computation based on perturbations. *Neural Computation*, 14(11):2531–2560, 2002. URL <http://doi.org/10.1162/089976602760407955>.

Manjunath, G. and Jaeger, H. Echo state property linked to an input: Exploring a fundamental characteristic of recurrent neural networks. *Neural Computation*, 25(3):671–696, 2013. URL http://doi.org/10.1162/NECO_a_00411. PMID: 23272918.

Marzen, Sarah. Difference between memory and prediction in linear recurrent networks. *Physical Review E*, 96(3):032308 [1–7], 2017. URL <http://doi.org/10.1103/PhysRevE.96.032308>.

Michael, Olivia, Obst, Oliver, Schmidsberger, Falk, and Stolzenburg, Frieder. RoboCupSimData: A RoboCup soccer research dataset. CoRR – Computing Research Repository <http://arxiv.org/abs/1711.01703>, Cornell University Library, 2017.

Michael, Olivia, Obst, Oliver, Schmidsberger, Falk, and Stolzenburg, Frieder. Analysing soccer games with clustering and conceptors. In *RoboCup 2017: Robot Soccer World Cup XXI. RoboCup International Symposium*, Nagoya, Japan, 2018. Springer. Available from <http://arxiv.org/abs/1708.05821>.

Neitzel, Rouven. Prediction of sinusoidal signals by recurrent neural networks. Project thesis, Automation and Computer Sciences Department, Harz University of Applied Sciences, 2018. In German.

Ollivier, Yann, Tallec, Corentin, and Charpiat, Guillaume. Training recurrent networks online without backtracking. CoRR – Computing Research Repository <http://arxiv.org/abs/1507.07680>, Cornell University Library, 2015.

Palangi, Hamid, Deng, Li, and Ward, Rabab K. Learning input and recurrent weight matrices in echo state networks. CoRR – Computing Research Repository [abs/1311.2987](http://arxiv.org/abs/1311.2987), Cornell University Library, 2013. URL <http://arxiv.org/abs/1311.2987>.

Pascanu, Razvan, Mikolov, Tomas, and Bengio, Yoshua. On the difficulty of training recurrent neural networks. *Proceedings of the 30th International Conference on Machine Learning*, 28(3):1310–1318, 2013. URL <http://proceedings.mlr.press/v28/pascanu13.pdf>.

Ragni, Marco and Klein, Andreas. Predicting numbers: An AI approach to solving number series. In Bach, Joscha and Edelkamp, Stefan (eds.), *KI 2011: Advances in Artificial Intelligence – Proceedings of the 34th Annual German Conference on Artificial Intelligence*, LNAI 7006, pp. 255–259, Berlin, 2011. Springer. URL http://doi.org/10.1007/978-3-642-24455-1_24.

Schmidhuber, Jürgen, Wierstra, Daan, Gagliolo, Matteo, and Gomez, Faustino. Training recurrent networks by evolino. *Neural Computation*, 19:757–779, 2007. URL <http://doi.org/10.1162/neco.2007.19.3.757>.

Steckhan, Kai. Time-series analysis with recurrent neural networks. Project thesis, Automation and Computer Sciences Department, Harz University of Applied Sciences, 2018. In German.

Stolzenburg, Frieder. Periodicity detection by neural transformation. In Van Dyck, Edith (ed.), *ESCOM 2017 – 25th Anniversary Conference of the European Society for the Cognitive Sciences of Music*, pp. 159–162, Ghent, Belgium, 2017. IPEM, Ghent University. URL <http://www.escom2017.org/wp-content/uploads/2016/06/Stolzenburg-et-al.pdf>. Proceedings.

White, Olivia L., Lee, Daniel D., and Sompolinsky, Haim. Short-term memory in orthogonal neural networks. *Physical Review Letters*, 92(14):148102, 1994. URL <http://journals.aps.org/prl/abstract/10.1103/PhysRevLett.92.148102>.

Xue, Yanbo, Yang, Le, and Haykin, Simon. Decoupled echo state networks with lateral inhibition. *Neural Networks*, 20(3):365–376, 2007. URL <http://doi.org/10.1016/j.neunet.2007.04.014>.